Characterization of a Small Metal Binding Protein from *Nitrosomonas europaea*†

Brett M. Barney,‡ Russell LoBrutto,§ and Wilson A. Francisco*,‡

Department of Chemistry and Biochemistry and the School of Life Sciences, Arizona State University, Tempe, Arizona 85287

Received April 6, 2004; Revised Manuscript Received July 6, 2004

ABSTRACT: A small metal-binding protein (SmbP) with no known similarity to other proteins in current databases was isolated and characterized from the periplasm of *Nitrosomonas europaea*. The primary structure of this small (9.9 kDa) monomeric protein is characterized by a series of 10 repeats of a seven amino acid motif and an unusually high number of histidine residues. The protein was isolated from *N. europaea* with Cu(II) bound but was found to be capable of binding multiple equivalents of a variety of divalent and trivalent metals. The protein was overexpressed in *Escherichia coli* and used for the study of its metal-binding properties by UV/vis, circular dichroism (CD), and electron paramagnetic resonance (EPR) spectroscopy and equilibrium dialysis and isothermal titration calorimetry. The protein was found to bind up to six Cu(II) atoms with dissociation constants of approximately 0.1 μM for the first two metal ions and approximately 10 μM for the next four. Binding of Cu(II) resulted in spectroscopic features illustrating two distinctive geometries, as determined by EPR spectroscopy. The levels of SmbP in the periplasm were found to increase by increasing the levels of copper in the growth media. This protein is proposed to have a role in cellular copper management in the ammonia-oxidizing bacterium *N. europaea*.

Copper is an essential element in living cells and is a cofactor in a large number of enzymes. It is also toxic at elevated concentrations, and several systems that regulate copper concentrations and confer copper resistance in a variety of organisms have been characterized (*1*, *2*). There are a variety of proteins that transport or facilitate copper efflux. These include the CopABCD and PcoABCD homologous systems of *Pseudomonas syringae* and *Escherichia coli*, respectively, which confer copper resistance to Gram-negative bacteria by sequestering copper in the periplasm and outer membrane (*3*, *4*). There are also a variety of copper chaperones (*5*) and copper transporters, such as the copper ATPases (*6*). Metallothioneins are a well-characterized diverse set of proteins that act as "metal sponges" and contain high numbers of cysteines (*3*, *5*). Another class of proteins that might have a role in copper regulation and sequestration in plants are the metallohistins, a new class of small histidine-rich proteins recently characterized, which are capable of binding multiple metal ions (*7*).

Recent genome sequencing projects have identified a large number of hypothetical proteins or proteins of unknown function from a variety of organisms. One key criterion in the selection of genomes for sequencing projects has been to choose organisms from unique environments, establishing a diverse source of genetic information, while also offering the opportunity to uncover new and novel proteins. One such organism is the ammonia-oxidizing bacterium *Nitrosomonas europaea*, which fills a specific niche as a chemoautolithotroph. This organism derives its energy requirements from the oxidation of ammonia to nitrite (for a recent review, see Arp et al. (*8*)). The genome of *N. europaea* has been recently sequenced (*9*).

We describe here the characterization of a novel small metal binding protein (SmbP)[1] isolated from the periplasm of *N. europaea* proposed to have a role in cellular copper management in this ammonia-oxidizing bacterium.

MATERIALS AND METHODS

Materials. Luria−Bertani (LB) broth was obtained from Fisher Biotech. Ni-NTA His·Bind resin was obtained from Novagen. Native and SDS−polyacrylamide gel electrophoresis were performed using equipment and reagents from Bio-Rad. Proteins were visualized with Coomassie Brilliant Blue R-250 (Bio-Rad). Plasmid purifications and isolations were done using the GenElute plasmid miniprep kit (Sigma). Genomic DNA was purified using the DNA isolation kit for cells and tissues from Roche Applied Science. $Vent_R$ DNA polymerase and restriction enzymes were obtained from New England BioLabs. Nucleotides were obtained as the PCR nucleotide mix from Roche Applied Science. DNA isolations from agarose gels were done using the QIAEX II gel extraction kit (Qiagen). Isopropyl-1-thio-β-D-galactopyranoside (IPTG) was obtained from Calbiochem and Benzonase nuclease was from Novagen. All other chemicals and

† B.M.B. was supported in part by a fellowship through the Research Training Grant in Optical Biomolecular Devices provided under a grant from the NSF (No. 9602258).

* To whom correspondence should be addressed. Tel: 480-965-7480. Fax: 480-965-2747. E-mail: wfrancisco@asu.edu.

‡ Department of Chemistry and Biochemistry.

§ School of Life Sciences.

[1] Abbreviations: SmbP, small metal binding protein; IPTG, isopropyl-1-thio-β-D-galactopyranoside; PDB, Protein Data Bank; LB, Luria−Bertani; PMSF, phenylmethylsulfonyl fluoride; Tris, 2-amino-2-(hydroxymethyl)-1,3-propanediol; DEAE, diethylaminoethyl; SDS, sodium dodecyl sulfate; PAGE, polyacrylamide gel electrophoresis; MES, 2-(*N*-morpholino)ethanesulfonic acid; HEPES, 4-(2-hydroxyethyl)piperazine-1-ethanesulfonic acid; PIPES, piperazine-1,4-bis(2-ethanesulfonic acid); EDTA, ethylenediaminetetraacetate; mT, millitesla; MALDI-TOF, matrix-assisted laser desorption time-of-flight.

10.1021/bi049318k CCC: $27.50
Published on Web 08/14/2004

biochemicals were of the highest purity available, purchased from Sigma-Aldrich, and were used without further purification. Oligomer synthesis and DNA sequencing were carried out by the DNA laboratory at Arizona State University.

Bacterial Strains and Growth Conditions. *Nitrosomonas europaea* (ATCC 19718) was obtained from the American Type Culture Collection. *Escherichia coli* DH5α competent cells were obtained from Life Technologies and *E. coli* BL21(DE3) cells were obtained from Novagen. *E. coli* cells were grown on LB broth at 30 °C. Kanamycin (30 μg/mL) was added for selection and maintenance of plasmid-containing clones. *N. europaea* was grown as described below.

Purification of SmbP from N. europaea. *N. europaea* was grown as previously described (*10*). To 1.5 L of autoclaved optimal growth media (50 mM $(NH_4)_2SO_4$, 48 mM K_2HPO_4, 2 mM NaH_2PO_4, 5 mM K_2CO_3, 1 mg/L cresol red, pH 8.0) in a 2 L baffled flask, 10 mL of a sterile metal salts solution was added to bring the media to 200 μM $CaCl_2$, 750 μM $MgCl_2$, 875 nM of $CuCl_2$, and 16 μM Fe-EDTA. The cultures were inoculated with a frozen stock of *N. europaea* cells and grown at 30 °C, while adding aqueous K_2CO_3 to maintain the pH above 7.0 until the culture reached stationary phase (~20 mM nitrite). Following growth, cells were harvested at 7000*g* for 7 min.

To prepare a periplasmic fraction, the following osmotic shock protocol was used. The harvested cells were resuspended in 20 mL of sucrose solution (30 mM Tris·HCl, pH 8.0, 20% sucrose) and 1.0 mM EDTA and incubated at 25 °C for 20 min with gentle stirring. The cells were pelleted at 10 000*g* for 7 min, and the supernatant was carefully removed. The pellet was resuspended in 2 mL of ice-cold 5 mM $MgSO_4$ solution and 10 μL of protease inhibitor cocktail (Sigma). The suspension was placed in 2 mL microcentrifuge tubes and pelleted at maximum speed (14 000 rpm) for 4 min, yielding the periplasmic fraction in the supernatant.

The supernatant was loaded onto a column (0.75 cm × 10 cm) of Ni-NTA His·Bind metal affinity resin (Novagen). The column was washed with one column volume of wash buffer (50 mM K_2HPO_4, 500 mM NaCl, 25 mM imidazole, pH 8.0) to remove unbound proteins, and SmbP was eluted with one column volume of elution buffer (50 mM K_2HPO_4, 500 mM NaCl, 500 mM imidazole, pH 8.0).

Expression of SmbP at Varied Copper Concentrations. Early work in our laboratory suggested that cellular concentrations of SmbP might fluctuate with copper concentrations in the growth media. In a controlled experiment, cultures were prepared as describe above without the inclusion of Cu(II). Copper was then added from a stock solution of $CuCl_2$ to a final concentration of 2.62 μM (high copper culture) or 0.875 μM (normal copper culture) and excluded from the no-copper culture. The relative amounts of SmbP and other periplasmic proteins were determined by SDS−PAGE.

Construction of SmbP Expression Vector pSMBP. The region upstream of the *smbP* gene (NCBI protein accession number NP_842452) and associated ribosomal binding site from *N. europaea* was amplified by PCR using the oligonucleotides 5′ GGAATT CCCCTG CGTATT CGCCGT GTTG 3′ and 5′ GGATAA CTCCGC TTTTGG TTGGC 3′ and genomic DNA isolated from *N. europaea*. The PCR product was isolated from an agarose gel, digested with *Eco*RI and *Hin*dIII (present downstream of *smbP* in the genomic sequence), and ligated into pET-30a(+) (Novagen) digested with the same enzymes. DNA was ligated with T4 DNA ligase. The new plasmid pSMBP was used to transform *E. coli* DH5α calcium chloride competent cells by heat shock (*11*). After 1 h of growth in 1 mL of LB media, the cells were pelleted and streaked onto LB plates containing kanamycin (30 μg/mL). Individual colonies were selected and analyzed by restriction digest to confirm correct plasmid incorporation. The plasmids were purified and transformed into *E. coli* BL21(DE3) calcium chloride competent cells by heat shock. Clones were isolated in the same manner as described above and used for expression. The clone selected for further work was sequenced to confirm the sequence.

Purification of Recombinant Protein. Cells of *E. coli* BL21(DE3) harboring the pSMBP plasmid were grown in 1.0 L of LB media containing kanamycin (30 μg/mL) at 25 °C. The cells were grown to an A_{600} of 0.5, induced with 50 mg of IPTG, grown for an additional 4 h, and harvested at 7000*g* for 7 min. Recombinant SmbP was purified as described above for the wild-type protein with some modifications required for the larger cell paste obtained with *E. coli*. A detailed purification protocol is included in Supporting Information. Apo-SmbP was prepared by dialyzing the purified protein against 5 mM EDTA in H_2O, followed by extensive dialysis against distilled water. It should be noted that SmbP has been stored for several weeks in deionized water without any noticeable degradation (as determined by SDS−PAGE).

Determination of Protein Concentration. The determination of the protein concentration by the absorbance at 280 nm is not possible because SmbP does not contain any aromatic residues. Quantitative amino acid analysis of purified SmbP was carried out at the Protein Laboratory Facility at Arizona State University, as described in Supporting Information. The amount of protein, as determined by amino acid analysis, indicated that the determination of the concentration of SmbP by the simple ultraviolet spectrophotometric analysis of Waddell (*12*) resulted in an overestimation of the protein concentration. The modified equation $90(A_{215} - A_{225})$ was routinely used for the determination of the concentration in micrograms per milliliter of SmbP in H_2O.

N-Terminal Sequencing, MALDI-TOF Mass Spectrometry, and Gel Filtration Chromatography. The N-terminal sequence of wild-type and recombinant SmbP was determined by Edman degradation. The molecular mass of SmbP was determined by MALDI-TOF mass spectrometry, and the molecular mass of SmbP under native conditions was determined by gel filtration chromatography (see Supporting Information).

Circular Dichroism (CD) of SmbP. CD spectra were obtained at 25 °C on a Jasco J710 spectropolarimeter. Experiments were carried out in water using cells of 1 mm path length for spectra recorded in the UV region (190−260 nm) and 1 cm path length for spectra recorded in the visible region (400−800 nm). The pH was maintained at 7.5 by adding small portions of 0.1 M NaOH or 0.1 M HCl. The addition of Cu(II) to apo-SmbP was performed using small aliquots from a stock aqueous solution of $CuCl_2$. All CD spectra are expressed as the difference in molar ellipticity ($\Delta\epsilon = \epsilon_l - \epsilon_r$; M^{-1} cm^{-1}).

Absorption Spectroscopy. UV−visible electronic absorption spectra were obtained on a Shimadzu UV 1601 double-beam spectrophotometer using 1 cm path-length quartz cuvettes. Measurements done in phosphate, Tris, PIPES, and HEPES resulted in either the precipitation of copper or spectroscopic interferences due to buffer−metal interactions, as determined by running controls with buffer and metal alone. To minimize these problems, UV−visible measurements were conducted in deionized water. Cu(II) and Fe(III) were chosen for spectroscopic absorption analysis because they exhibit distinct spectral features when added to SmbP. The addition of metal ions to apo-SmbP was performed using small aliquots from stock aqueous solutions of $CuCl_2$ or $FeCl_3$. The pH was maintained at 7.5 by adding small portions of 0.1 M NaOH or 0.1 M HCl.

Equilibrium Dialysis Experiments. Cu(II)-binding measurements by equilibrium dialysis were conducted following a modification of the method of Jensen et al. (*13*). A detailed experimental protocol is included in Supporting Information.

Isothermal Titration Calorimetry. SmbP titrations with Cu(II) were performed on a MicroCal OMEGA calorimeter at 30 °C. Solutions of 100−150 μM of SmbP in either 30 mM MOPS (pH 7.5) or 30 mM MES (pH 7.0) were titrated with 10 mM aqueous $CuCl_2$ in H_2O. The reaction cell contained 1.5 mL of the protein solution in buffer. Cu(II) was added in 1.5 μL increments at 180 s intervals. Blank injections of metal solution in H_2O into corresponding buffer in the absence of protein were used to account for the heats of mixing and dilution. The binding constants were estimated from the obtained isotherms using the calorimetric analysis program Origin and were fit to two sets of independent sites because this provided the best fit for the data.

Electron Paramagnetic Resonance (EPR) Spectroscopy. Wild-type and recombinant SmbP were analyzed by EPR spectroscopy. Samples of apo-SmbP were titrated with increasing equivalents of Cu(II) from a stock solution of $CuCl_2$. Once the metal was bound to the protein (as indicated by the change in color after several seconds), 50 mM HEPES, pH 7.5, was added to each sample to maintain the pH. Alternatively, samples of apo-SmbP in 50 mM *N*-ethylmorpholine, pH 7.8, were titrated with increasing equivalents of Cu(II). EPR spectra were recorded on a Bruker Elexsys 580 spectrometer at 125 K. The wild-type sample spectrum was obtained as an average of 30 scans over the region from 240 to 360 mT, using a microwave power of 1.0 mW, a modulation amplitude of 0.8 mT, a time constant of 81.92 ms, and a microwave frequency of 9.41 GHz. Spectra of recombinant SmbP were obtained as an average of two scans over the region from 240 to 460 mT using the same parameters.

RESULTS

SmbP is a Monomeric Periplasmic Protein. A small abundant soluble protein of unknown function (NCBI accession number NP_842452) was isolated and purified from *N. europaea*. Protein sequencing revealed that the amino-terminal sequence of this protein (SGHTAHVDEAV) matched a region of 24 amino acids downstream of the putative N-terminus of an unknown protein from the genome of *N. europaea* (NCBI accession number NP_842452) (*9*), possibly indicating that the gene included a cleaved leader sequence that might direct it to the periplasm. This result correlated well with the predicted results from the signalP server (*14*, *15*). The cellular location was confirmed by isolation of the protein from the periplasm of *N. europaea*.

A. SmbP Sequence (following N-terminal cleavage)

```
SGHTAHVDEAVKHAEEAVAHGKEGHTDQLLEHAKE
SLTHAKAASEAGGNTHVGHGIKHLEDAIKHGEEGH
VGHATKHAQEAIEHLRASHEKSH
```

B. Ten Sets of Seven Residue Repeats

```
SG[HTAHVDE][AVKHAEE][AVAHGKE]GHTDQ-
          [LLEHAKE][SLTHAKA]ASEAG-
   [GNTHVGH][GIKHLED][AIKHGEE]GHVGH-
          [ATKHAQE][AIEHLRA]SHEKSH
```

FIGURE 1: SmbP primary sequence analysis: (A) illustration of the primary sequence for the SmbP protein following the N-terminal cleavage of the leader sequence that directs SmbP to the periplasm; (B) depiction of the 10 sets of repeated amino acid residues from the sequence, which make up the highly conserved seven residue motif.

The mature peptide is 93 amino acids in length. The molecular mass of the protein as determined by MALDI-TOF mass spectrometry (9866 Da) is in perfect agreement to the theoretical value of 9865.6 Da. SmbP was determined to be monomeric by gel filtration chromatography. In a Sephadex G-75 column, SmbP elutes after carbonic anhydrase (29 kDa) and before aprotinin (6.5 kDa) but coelutes with cytochrome *c* (12.4 kDa) (results not shown). The same elution profiles were obtained in the absence and presence of Cu(II) in the buffer. The formation of oligomeric forms of SmbP was not detected under these conditions.

This unique protein is distinguished by 10 sequential repeats of a seven amino acid motif characterized by an absolutely conserved histidine residue in the fourth position and conserved residues at each of the other six positions (Figure 1). Extensive searches of the current databases did not identify any proteins with significant homology. The protein, as isolated from *N. europaea*, had approximately one copper atom bound per protein molecule.

SmbP is characterized by an unusually high number of histidine residues (17%). The apoprotein has negligible absorbance between 260 and 280 nm resulting from the lack of tryptophan, tyrosine, and phenylalanine residues. The protein also does not contain any methionine or cysteine residues. Besides histidine, the protein is primarily an assembly of alanine (16%), glutamate (14%), glycine (11%), and lysine (9%), accounting for 67% of the amino acid composition. The percentage of nonpolar amino acids is also very low, although a nonpolar residue is the predominant amino acid for the second position of the seven-unit repeat and likely contributes to the stabilization of a hydrophobic core. The protein is simple in design and nature, and secondary structure predictions suggest that the protein is a four α-helix bundle (*16*−*18*), corresponding closely with the four sets of repeats depicted in part B of Figure 1.

SmbP was cloned into *E. coli* to provide the larger quantities of protein required for spectroscopic studies. It was found that *E. coli* also processes the protein, cleaving the leader sequence and transporting the mature protein to the periplasm. Osmotic shock, followed by nickel affinity chromatography, yields quantities greater than 50 mg of highly purified recombinant SmbP per liter of cells (Figure S1).

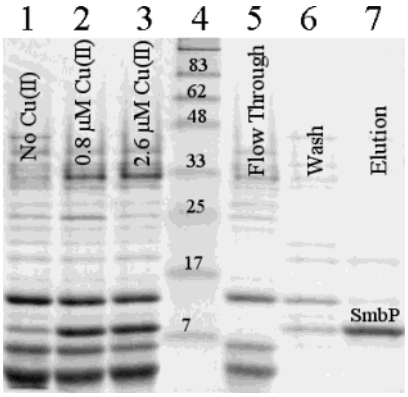

FIGURE 2: Periplasmic levels of SmbP. The level of SmbP (just above 7 kDa standard) in the periplasmic fraction from cultures grown with no added copper (lane 1) are noticeably lower than the levels under normal (0.8 μM) and high copper (2.6 μM) concentrations (lane 2 and 3). SmbP binds tightly to metal chelating affinity columns and elutes under high imidazole concentrations (250 mM) (lane 7). Lane 4 is a New England Biolabs prestained protein standard with the bands labeled in kDa.

Cellular Levels of SmbP Are Affected by Copper Concentration. As isolated from *N. europaea*, SmbP was found to contain bound copper. To determine whether the levels of copper in the growth media affect the concentration of SmbP, an experiment was conducted in which *N. europaea* was grown at varying concentrations of Cu(II) and the relative amounts of SmbP in the periplasmic fraction were determined by SDS−PAGE. In this experiment, cultures of *N. europaea* were grown under the same conditions except for copper levels in the media. SDS−PAGE gels of the periplasmic proteins obtained at various Cu(II) concentrations are shown in Figure 2. While protein bands above and below SmbP were found in similar concentrations, independent of the copper concentration, the amount of SmbP is noticeably lower in the culture grown without addition of copper. The weight of cell paste obtained for the three conditions was approximately the same, suggesting that the absence of copper in the media (besides basal levels) did not significantly affect cell growth. Further studies indicated that while the concentration of SmbP in the cell was minimal at concentrations of Cu(II) below 100 nM copper, the amount of SmbP began to increase when levels above 300 nM Cu(II) were added to the media (results not shown).

Circular Dichroism of SmbP Confirms an α-Helical Structure. Predictions of the secondary structure of SmbP suggest a predominantly α-helical structure. To confirm this prediction, circular dichroism studies in the UV region were conducted on samples of SmbP in the absence and presence of Cu(II) at pH 7.5. The results indicate that the protein is comprised primarily of α-helices, as determined by the presence of the two peak minima at 208 and 222 nm (Figure 3A). Analysis of the CD spectrum using the program Selcon3 in Dichroweb (*19*, *20*) suggests approximately 69% helical content, correlating well with predicted results from the PROFsec secondary structure prediction programs (∼68%) (*16*, *17*). The near-UV CD spectra of the apo- and copper-bound SmbP at pH 7.5 are similar (Figure 3A). The only difference observed is a small increase in the intensity of the positive CD band at 192 nm, indicating that Cu(II) binding to SmbP increases the helicity of SmbP. Analysis of the UV CD spectra of apo- and Cu(II)-bound SmbP using

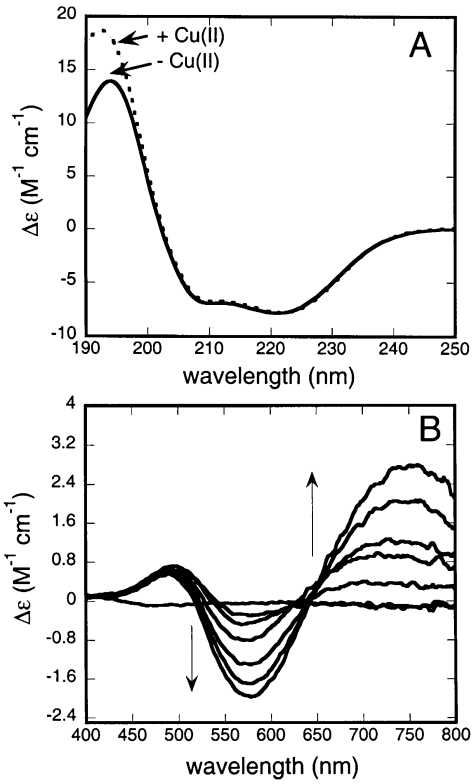

FIGURE 3: Panel A shows the UV CD spectra (190−250 nm) of apo-SmbP and SmbP (25 μM, pH 7.5, no buffer) with 1 equiv of Cu(II) bound. Spectra for 2 and 5 mol equiv of Cu(II) are not shown because they are virtually identical to the 1 mol equiv of Cu(II). Panel B shows the visible CD spectra (400−800 nm) of SmbP (250 μM, pH 7.5, no buffer) titrated with increasing equivalents of Cu(II) (0, 0.8, 1.4, 2.7, 3.7, 4.6, and 5.3) from an aqueous solution of $CuCl_2$. Additional mole equivalents of Cu(II) did not result in further changes in the CD spectra.

the program Selcon3 in Dichroweb (*19*, *20*) indicates an increase in the α-helical content following Cu(II) binding from approximately 65% to 76%.

Metal Binding Spectroscopic Features. Apo-SmbP is devoid of any spectroscopic signal above 260 nm. Titration of apo-SmbP with Cu(II) resulted in an absorption feature centered at 260 nm that increased linearly through approximately 6 equiv of copper (Figure S2). The addition of Cu(II) also led to changes in the spectral features between 400 and 800 nm (Figure 4). In this region, addition of copper led first to a feature centered at 550 nm for the first 2 equiv and a second feature centered near 625 nm for increasing equivalents. The change in absorbance in this region was found to also increase linearly through the same 6 equiv of metal, while addition of excess copper did not result in a further significant increase. The extinction coefficient at 625 nm for the fully Cu(II)-loaded protein is 420 M^{-1} cm^{-1} (with an average of 70 typical of a type II Cu(II) d−d transition (*21*).

CD experiments in the visible region were conducted with SmbP at increasing concentrations of copper. When Cu(II) is added to apo-SmbP, CD bands arising due to d−d transitions and $N_{imidazole}$ to Cu(II) charge transfer appear in the visible region (Figure 3B). After the addition of 1 equiv of Cu(II), a positive CD band at 490 nm and a negative CD band at 578 nm are observed. Addition of increasing equivalents of Cu(II) resulted in an increase in the intensity of the CD band at 578 nm and the appearance of a new broad

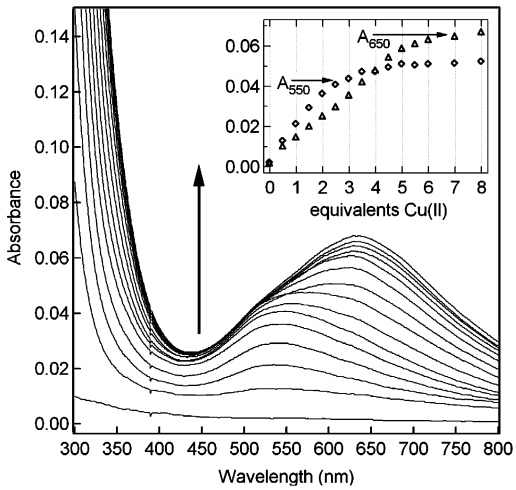

FIGURE 4: Absorbance changes resulting from copper(II) titration of SmbP. Absorption spectra of recombinant SmbP (167 μM) titrated with increasing equivalents of Cu(II) are shown. A plot of the absorbance at 550 and 650 nm versus increasing equivalents of Cu(II) is shown in the inset.

positive CD band at 760 nm. The intensity of the band at 490 nm does not increase with increasing equivalents of Cu(II), but the bands at 578 and 760 nm increase in intensity until approximately 6 equiv of Cu(II) has been added. These transitions become observable by CD only when Cu(II) is in a chiral ligand environment, and thus trace amounts of aqueous copper ions are not detected.

Fe(III) was also selected for the characterization of the metal binding properties of SmbP by UV/vis spectroscopy. Titration of recombinant SmbP with Fe(III) resulted in two absorption features centered at 260 and 355 nm, respectively, that increased linearly through approximately 6 equiv of iron (results not shown). After 6 equiv, further addition of Fe(III) did not result in additional increase in the intensity of these peaks, indicating that at least six Fe(III) ions are bound to SmbP.

Measurements of Cu(II) Binding to SmbP. Dialysis experiments were conducted to determine the Cu(II) to protein binding ratio under equilibrium conditions. Under these conditions, SmbP reached a binding capacity of two to three Cu(II) ions per SmbP molecule. This value is smaller than that determined by UV/vis spectroscopy and did not allow a precise determination of the binding constant (results not shown).

To further examine the nature of Cu(II) binding and to determine the binding constants of the various metal-binding sites on SmbP for Cu(II), isothermal titration calorimetry studies were conducted (Figure 5). These experiments were performed in MES (pH 7.0) and MOPS buffer (pH 7.5) because both buffers have been shown to have negligible interference with copper. Samples of buffer alone were also titrated to subtract the background difference related to the buffer. The resulting isotherms were fit to a model for two sets of sites using the program Origin. Data were fit by several suggested methods, either forcing the values for n (number of metals per site) to whole numbers (2 for the first site) or by using the protein concentration determined spectrophotometrically. In each case, significant differences were found between the binding constants of the two sets of sites. For the high-affinity site, values of K_1 ranged from

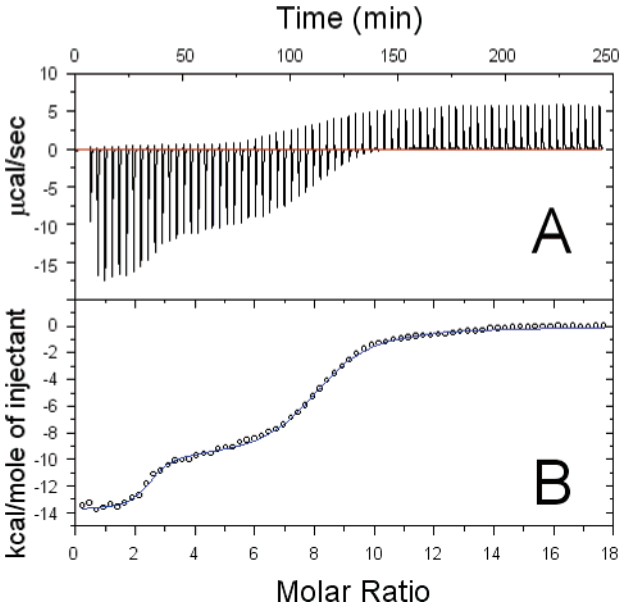

FIGURE 5: Calorimetric titration of SmbP with Cu(II): (A) raw data for 1.5 μL injections of 10 mM copper chloride into the reaction containing 1.5 mL of 100 μM SmbP in 30 mM MOPS, pH 7.5; (B) integrated data after subtraction of a control experiment in the absence of protein. Curve fitting was performed by a sequential iterative fit of the thermodynamic parameters to two sets of sites using the program Origin. Exclusion of the first data point resulted in an improvement in the standard errors of the iterative fit.

0.55×10^7 to 1.4×10^7 M^{-1} and reaction enthalpies, ΔH_1, ranged from -1.3×10^4 to -1.4×10^4 cal/mol. For the lower affinity site, values of K_2 ranged from 0.59×10^5 to 2.5×10^5 M^{-1}, and reaction enthalpies, ΔH_2, ranged from -0.9×10^4 to -1.0×10^4 cal/mol. These values included fits where the number of metal atoms per site were forced to 2 (1.97 actual) and 5 (4.79 actual), while in other fits, they resulted in approximately 2.4 and 5.5 sites, allowing for the best possible fit. The ratio of the equilibrium constants for the two sites is approximately 100, indicating a significant difference in the affinities of the two sites. The two sites display negative cooperativity based on the biphasic features of data.

EPR Characterization of Metal Binding Sites. The EPR spectrum of wild-type *N. europaea* SmbP required 30 scans to refine the spectra from background noise. By comparison, the spectrum of recombinant SmbP dialyzed against copper only required two scans because the concentration of Cu(II) in this sample was much higher. However, the spectra obtained for the two proteins did not overlay well. The origin of this difference was determined by preparing samples of apo-SmbP titrated with increasing equivalents of Cu(II) (Figure 6). A good match between the spectra of wild-type and recombinant protein was found when only one or two copper ions were bound per molecule of SmbP. The results also indicate a clear difference between at least two separate and distinct copper binding sites.

Spin integration of the EPR spectra versus equivalents of Cu(II) added, shown as an inset in Figure 6B, shows that the signal intensity increases linearly up to 6−8 equiv of Cu(II), confirming the binding stoichiometry of Cu(II) to SmbP. The addition of further mole equivalents results in no further increase in the intensity of the EPR spectra. Cu(II) ions in H_2O at pH > 7 give a largely EPR silent signal (*22*)

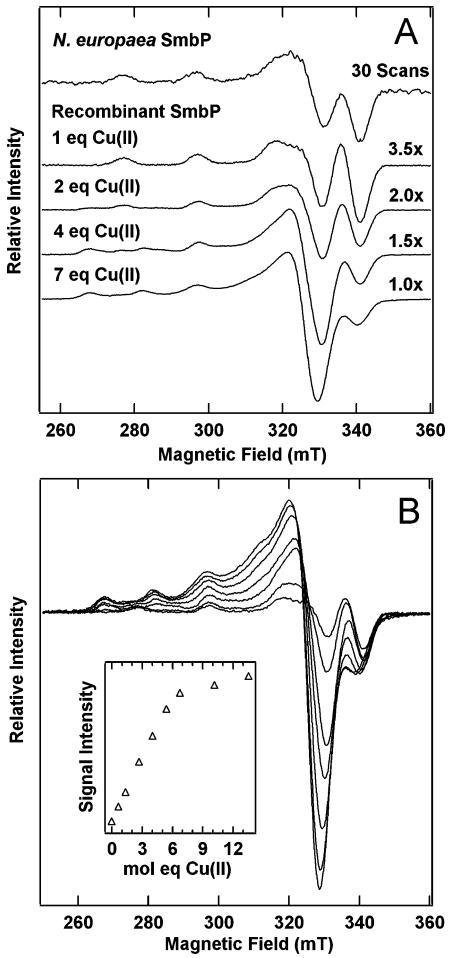

FIGURE 6: EPR analysis of copper(II)−SmbP: (A) EPR spectra of *N. europaea* SmbP as isolated (top spectrum) and recombinant apo-SmbP (300 μM) from *E. coli* titrated with different mole equivalents of Cu(II) (1, 2, 4, and 7); (B) SmbP (300 μM) in 50 mM *N*-ethylmorpholine, pH 7.8, titrated with increasing equivalents of Cu(II) (0, 0.7, 1.4, 2.7, 4.0, 5.4, 6.8, 10.2, and 13.6). Double integration of EPR spectra plotted versus mole equivalents of Cu(II) to SmbP (inset) indicates that saturation occurs at approximately 6−8 mol equiv of Cu(II).

and Cu(II) ions in *N*-ethylmorpholine buffer at pH 7.8 result in dramatically attenuated EPR signals relative to Cu(II) bound to SmbP, as has been previously reported for the binding of Cu(II) to the amyloid-β peptide (*23*).

To further define the electronic features of the two types of metal binding sites, simulations of the EPR spectra were done using the updated version of the program QPOW (*24*−*26*). The EPR spectrum of SmbP with only 1 equiv of bound copper was used for the first simulation. The simulation of this spectrum yielded values for a rhombic center with $g_x = 2.062$, $g_y = 2.025$, $g_z = 2.195$, $A_\perp = 2.5$ mT, and $A_\parallel = 21.4$ mT (Figure S3). These spectral features are similar to those of model square-planar 4N geometries (*27*, *28*) and related to a biuret form of copper (*29*), indicating a square-planar geometry with four nitrogen ligands. The simulation of the second site was done using the difference spectra between 4 and 2 equiv of copper bound. This spectra yielded values for axial centers of $g_\perp = 2.06$, $g_\parallel = 2.32$, $A_\perp = 0.5$ mT, and $A_\parallel = 17.1$ mT (Figure S3). These parameters are indicative of three nitrogen/one oxygen or two nitrogen/two oxygen ligands with tetragonal symmetry (*30*).

DISCUSSION

A small periplasmic metal binding protein (SmbP) was isolated from *Nitrosomonas europaea* by metal affinity chromatography. This protein was sequenced and determined to be the mature form of a small protein with an unusually high percentage of histidine residues (17%). The protein has a unique sequence with no homology to any other protein in current databases. In addition to the large number of histidines, it contains a high number of acidic residues, as well as alanine and glycine, but lacks any aromatic or sulfur-containing residues. A deeper investigation of the primary sequence of the protein revealed a repeating motif of seven amino acids with histidine as the absolutely conserved fourth residue. Secondary structure predictions indicated that SmbP likely consists of four α-helical bundles, most likely corresponding to the four regions of the repeated motif shown in part B of Figure 1.

The protein was of particular interest because it is unique to this organism. A protein BLAST search (*31*) of the more than 140 bacterial genomes currently available did not identify any protein with significant similarity. Analysis of the periplasmic fraction of *N. europaea* revealed that this protein is produced in high quantities (one of the four strongest bands in lanes 2 and 3 of Figure 2), and additional experiments with *N. europaea* revealed that the levels of SmbP decreased when low concentrations of copper were used in the growth media. Concentrations of SmbP in the periplasmic fraction drop dramatically when only background levels of Cu(II) (below 300 nM) are added to the media during growth of the organism.

SmbP was cloned into *E. coli* to provide larger quantities of protein. *E. coli* also processes the protein, cleaving the leader sequence and transporting the mature protein to the periplasm. Osmotic shock, followed by nickel affinity chromatography, yields quantities greater than 50 mg of highly purified recombinant SmbP per liter of cells. The protein had to be dialyzed against EDTA to remove any residual metals picked up during growth or purification from the metal affinity step. EPR and CD spectra of apo-SmbP show no Cu(II)-associated signals, confirming that all associated Cu(II) can be removed by dialysis with EDTA. Recombinant SmbP was used in spectroscopic and calorimetric studies to characterize the metal binding properties of the protein.

Spectroscopic investigation of the metal binding properties of SmbP revealed that the protein is able to bind multiple metal atoms including Mn^{2+}, Ni^{2+}, Mg^{2+}, and Zn^{2+}, in addition to Cu^{2+} and Fe^{3+}, while it seemed to be nonspecific for cobalt (results not shown). The metal binding stoichiometry of SmbP was determined by a number of techniques. Upon addition of Cu(II) and Fe(III), an absorption band in the 250−260 nm region is observed, as well as ones in the 450−800 and 310−500 nm region for Cu(II) and Fe(III), respectively, increasing linearly through 6 equiv of metal, indicating that the protein is able to bind a minimum of six metal ions per protein molecule. CD bands in the visible region due to d−d transitions and $N_{imidazole}$ to Cu(II) charge transfer are also observed upon addition of Cu(II) to SmbP.

Isothermal titration calorimetry experiments of SmbP with Cu(II) in several buffer systems yielded isotherms with two phases. These results indicate negative cooperativity for the

binding of metal to two different sites. The results were fit to a model yielding dissociation constants of 0.07−0.2 μM for the first 2 equiv and 4−16 μM for the next 4−5 equiv of metal. In addition, equilibrium dialysis experiments corroborated that SmbP contains a high-affinity binding site with a dissociation constant in the low micromolar range. The inability to observe the binding of the additional four to five copper ions to SmbP by equilibrium dialysis might be related to a competition between these low-affinity binding sites and Chelex 100, which has been shown to deplete the sample of copper given sufficient time.

Spectroscopic studies have shown that the observed metal binding sites have different geometries. SmbP binds the first 2 equiv of copper selectively and with high affinity to a rhombic site with parameters of $g_{||}$ and $A_{||}$ suggesting four nitrogen ligands based on the Peisach−Blumberg plot (*30*) and studies of model compounds (*27*). The observed absorption peak near 550 nm is indicative of nitrogen ligand field (d−d) transitions and theoretical shifts in energy of d orbital states related to square-planar geometries (*32*). Subsequent copper atoms bind with lower affinity to an axial site indicative of three nitrogen/one oxygen or two nitrogen/two oxygen ligands with tetragonal symmetry based on the Peisach−Blumberg plot (*30*). The absorption at higher wavelengths, centered near 625 nm, is also indicative of mixed ligands (*32*). While this protein is not classified as a blue-copper protein, due to the lack of a cysteine residue as a ligand, SmbP exhibits a weak blue absorbance value due to ligand field (d−d) transitions ($\epsilon_{625} = 420$ M^{-1} cm^{-1} for the fully loaded protein), which is weaker than the charge-transfer transition absorption feature seen in the UV region ($\epsilon_{260} = 13\,700$ M^{-1} cm^{-1}).

Mature SmbP is devoid of sulfur-containing amino acids but has an unusually high percentage of alanine. In addition, SmbP contains a large number of histidines (16) and acidic residues (3 aspartates and 16 glutamates) that could serve as ligands for the multiple atoms of copper that bind to the protein. SmbP differs from other copper binding proteins, which utilize common motifs that include cysteine or methionine ligands (*5*). Although proteins with significant homology have not been identified, two types of proteins with an unusual number of histidine residues able to bind multiple metal ions have been described. The metallohistins are plant-derived periplasmic small multimeric histidine-rich proteins capable of binding multiple atoms of Zn^{2+}, Ni^{2+}, Co^{2+}, Cu^{2+}, Cd^{2+}, and Hg^{2+} (*7*). Unlike SmbP, metallohistins are predominantly composed of β-sheets, and the polypeptide sequence of the mature protein contains three distinct regions: an amino acid region rich in glutamate and aspartate residues, a glycine- and histidine-rich domain, and a glutamate-rich C-terminal domain (*7*). The histatins are small histidine-rich salivary peptides (24−38 aa) with a high content of tyrosine and acidic amino acids. Histatins have high affinity for Zn^{2+} and Cu^{2+} and contain three distinct binding sites with different affinities for these two metal ions (*33*).

The mechanism for copper homeostasis in *N. europaea* has not been studied and is not yet understood. Analysis of the genomic data suggests that the organism contains homologues of proteins known to participate in copper transport and storage similar to those that have been identified in other bacteria in which the mechanism of copper homeostasis is better understood, including *E. coli* (*34*), *Enterococcus hirae* (*35*), and *Pseudomonas syringae* (*3*). These include a copper ion transport ATPase (NE1019), three copper resistance proteins A, B, and C (NE0279, NE0280, and NE2058), a copper binding protein CopC (NE1491), and an inner membrane copper tolerance protein (NE2389) (*9*). Unlike in *E. coli*, these genes do not appear in clusters. SmbP may prove to be an addition to the assortment of periplasmic proteins known to be important in the trafficking and sequestering of metal atoms such as copper (*5*). The failure to find a homologous protein in other organisms might indicate a specialized role for the protein in the cell and might be related to the unique and specialized niche filled by the obligate chemolithotroph *N. europaea*, which obtains its energy for growth from the oxidation of ammonia to nitrite through the copper-containing ammonia monooxygenase (*8*).

With regards to protein design, four-helix bundles have been extensively used as models for understanding protein folding and function and have been used as templates for de novo design of metal binding sites (*36*, *37*). SmbP, proposed to fold as a four-helix bundle, is capable of binding a large number of metal ions. We expect that further structural studies with this protein should provide important insight into the field of protein folding and metalloprotein design, and the determination of the solution structure and protein folding experiments are currently underway.

The high amounts of SmbP found in the periplasm of the cell indicate an important role for the protein, while the simple framework of repeating motifs, relative stability over a broad range of conditions, and specificity of the binding make it an interesting protein for further study. Based on the findings from these studies, SmbP is proposed to be a metal scavenging protein in *N. europaea*, induced to deal with high concentrations of copper.

ACKNOWLEDGMENT

We thank Jeremy Lewis for assistance with protein purification and circular dichroism analysis. We also thank R. L. Belford, A. M. Maurice, and M. J. Nilges for the use of the program QPOW and Dr. Joshua Telser for the updated version of QPOW used in this work to simulate EPR spectra. Daniel Brune and John Lopez are acknowledged for MALDI-TOF MS analysis and amino-terminal sequencing. The Voyager DE STR mass spectrometer used by the Protein Laboratory Facility at Arizona State University was purchased under NSF Grant CHE-0131222.

SUPPORTING INFORMATION AVAILABLE

Detailed experimental procedures, SDS−PAGE of recombinant SmbP, simulations of EPR spectra, and Cu(II)-titration plots in the UV region. This material is available free of charge via the Internet at http://pubs.acs.org.

REFERENCES

1. Outten, F. W., Huffman, D. L., Hale, J. A., and O'Halloran, T. V. (2001) The independent *cue* and *cus* systems confer copper tolerance during aerobic and anaerobic growth in *Escherichia coli*, *J. Biol. Chem. 276*, 30670−30677.
2. Huffman, D. L., Huyett, J., Outten, F. W., Doan, P. E., Finney, L. A., Hoffman, B. M., and O'Halloran, T. V. (2002) Spectroscopy of Cu(II)-PcoC and the multicopper oxidase function of PcoA, two essential components of *Escherichia coli* pco copper resistance operon, *Biochemistry 41*, 10046−10055.

3. Silver, S., and Ji, G. G. (1994) Newer systems for bacterial resistances to toxic heavy metals, *Environ. Health Perspect. 102*, 107−113.
4. Arnesano, F., Banci, L., Bertini, I., Mangani, S., and Thompsett, A. R. (2003) A redox switch in CopC: An intriguing copper trafficking protein that binds copper(I) and copper(II) at different sites, *Proc. Natl. Acad. Sci. U.S.A. 100*, 3814−3819.
5. Wernimont, A. K., Huffman, D. L., Finney, L. A., Demeler, B., O'Halloran, T., and Rosenzweig, A. C. (2003) Crystal structure and dimerization equilibria of PcoC, a methionine-rich copper resistance protein from *Escherichia coli*, *J. Biol. Inorg. Chem. 8*, 185−194.
6. Lu, Z. H., Cobine, P., Dameron, C. T., and Solioz, M. (1999) How cells handle copper: A view from microbes, *J. Trace Elem. Exp. Med. 12*, 347−360.
7. Gupta, R. K., Dobritsa, S. V., Stiles, C. A., Essington, M. E., Liu, Z. Y., Chen, C. H., Serpersu, E. H., and Mullin, B. C. (2002) Metallohistins: A new class of plant metal-binding proteins, *J. Protein Chem. 21*, 529−536.
8. Arp, D. J., Sayavedra-Soto, L. A., and Hommes, N. G. (2002) Molecular biology and biochemistry of ammonia oxidation by *Nitrosomonas europaea*, *Arch. Microbiol. 178*, 250−255.
9. Chain, P., Lamerdin, J., Larimer, F., Regala, W., Lao, V., Land, M., Hauser, L., Hooper, A., Klotz, M., Norton, J., Sayavedra-Soto, L., Arciero, D., Hommes, N., Whittaker, M., and Arp, D. (2003) Complete genome sequence of the ammonia-oxidizing bacterium and obligate chemolithoautotroph *Nitrosomonas europaea*, *J. Bacteriol. 185*, 2759−2773.
10. Hyman, M. R., and Arp, D. J. (1992) $^{14}C_2H_2$-Labeling and $^{14}CO_2$-labeling studies of the denovo synthesis of polypeptides by *Nitrosomonas europaea* during recovery from acetylene and light inactivation of ammonia monooxygenase, *J. Biol. Chem. 267*, 1534−1545.
11. Ausubel, F. M., Ed. (1998) *Current Protocols in Molecular Biology*, Wiley, New York.
12. Waddell, W. J. (1956) A simple ultraviolet spectrophotometric method for the determination of protein, *J. Lab. Clin. Med. 48*, 311−314.
13. Jensen, P. Y., Bonander, N., Horn, N., Tumer, Z., and Farver, O. (1999) Expression, purification and copper-binding studies of the first metal-binding domain of Menkes protein, *Eur. J. Biochem. 264*, 890−896.
14. Nielsen, H., Engelbrecht, J., Brunak, S., and vonHeijne, G. (1997) Identification of prokaryotic and eukaryotic signal peptides and prediction of their cleavage sites, *Protein Eng. 10*, 1−6.
15. Nielsen, H., Brunak, S., and von Heijne, G. (1999) Machine learning approaches for the prediction of signal peptides and other protein sorting signals, *Protein Eng. 12*, 3−9.
16. Rost, B., and Sander, C. (1994) Combining evolutionary information and neural networks to predict protein secondary structure, *Proteins 19*, 55−72.
17. Rost, B., and Sander, C. (1993) Prediction of protein secondary structure at better than 70- percent accuracy, *J. Mol. Biol. 232*, 584−599.
18. Combet, C., Blanchet, C., Geourjon, C., and Deleage, G. (2000) NPS@: Network Protein Sequence Analysis, *Trends Biochem. Sci. 25*, 147−150.
19. Lobley, A., Whitmore, L., and Wallace, B. A. (2002) DICHROWEB: an interactive website for the analysis of protein secondary structure from circular dichroism spectra, *Bioinformatics 18*, 211−212.
20. Lobley, A., and Wallace, B. A. (2001) Dichroweb: A website for the analysis of protein secondary structure from circular dichroism spectra, *Biophys. J. 80*, 373A.
21. Fawcett, T. G., Bernarducci, E. E., Kroghjespersen, K., and Schugar, H. J. (1980) Charge-transfer absorptions of Cu(II)-Imidazole and Cu(II)-imidazolate chromophores, *J. Am. Chem. Soc. 102*, 2598−2604.
22. Aronoff-Spencer, E., Burns, C. S., Avdievich, N. I., Gerfen, G. J., Peisach, J., Antholine, W. E., Ball, H. L., Cohen, F. E., Prusiner, S. B., and Millhauser, G. L. (2000) Identification of the Cu^{2+} binding sites in the N-terminal domain of the prion protein by EPR and CD spectroscopy, *Biochemistry 39*, 13760−13771.
23. Syme, C. D., Nadal, R. C., Rigby, S. E. J., and Viles, J. H. (2004) Copper binding to the amyloid-beta (A beta) peptide associated with Alzheimer's disease − Folding, coordination geometry, pH dependence, stoichiometry, and affinity of A beta-(1−28): Insights from a range of complementary spectroscopic techniques, *J. Biol. Chem. 279*, 18169−18177.
24. Nilges, M. J. (1979) Electron paramagnetic resonance studies of low symmetry nickel(I) and molybdenum(V) complexes, Ph.D. Thesis, University of Illinois, Urbana, Illinois.
25. Maurice, A. M. (1980) Acquisition of anisotropic information by computational analysis of isotropic EPR spectra, Ph.D. Thesis, University of Illinois, Urbana, Illinois.
26. Bedford, R. L., and Nilges, M. J. (1979) Computer Simulation of Powder Spectra, in *EPR Symposium, 21st Rocky Mountain Conference*, Denver, CO.
27. Scholl, H. J., and Huttermann, J. (1992) ESR and ENDOR of Cu(II) complexes with nitrogen donors: Probing parameters for prosthetic group modeling of superoxide dismutase, *J. Phys. Chem. 96*, 9684−9691.
28. Aasa, R., and Aisen, P. (1968) An electron paramagnetic resonance study of iron and copper complexes of transferrin, *J. Biol. Chem. 243*, 2399−2404.
29. Rotilio, G., Finazzia, A., Calabres, L., Bossa, F., Guerrier, P., and Mondovi, B. (1971) Studies of metal sites of copper proteins. 2. Ligands of copper in hemocuprein, *Biochemistry 10*, 616−621.
30. Peisach, J., and Blumberg, W. E. (1974) Structural implications derived from analysis of electron- paramagnetic resonance-spectra of natural and artificial copper proteins, *Arch. Biochem. Biophys. 165*, 691−708.
31. Altschul, S. F., Madden, T. L., Schaffer, A. A., Zhang, J. H., Zhang, Z., Miller, W., and Lipman, D. J. (1997) Gapped BLAST and PSI-BLAST: a new generation of protein database search programs, *Nucleic Acids Res. 25*, 3389−3402.
32. Solomon, E. I., Penfield, K. W., and Wilcox, D. E. (1983) Active sites in copper proteins. An electronic structure overview, *Struct. Bonding 53*, 1−57.
33. Gusman, H., Lendenmann, U., Grogan, J., Troxler, R. F., and Oppenheim, F. G. (2001) Is salivary histatin 5 a metallopeptide? *Biochim. Biophys. Acta-Protein Struct. Mol. Enzymol. 1545*, 86−95.
34. Rensing, C., and Grass, G. (2003) *Escherichia coli* mechanisms of copper homeostasis in a changing environment, *FEMS Microbiol. Rev. 27*, 197−213.
35. Solioz, M., and Stoyanov, J. V. (2003) Copper homeostasis in *Enterococcus hirae*, *FEMS Microbiol. Rev. 27*, 183−195.
36. Schnepf, R., Horth, P., Bill, E., Wieghardt, K., Hildebrandt, P., and Haehnel, W. (2001) De novo design and characterization of copper centers in synthetic four-helix-bundle proteins, *J. Am. Chem. Soc. 123*, 2186−2195.
37. Hill, R. B., Raleigh, D. P., Lombardi, A., and DeGrado, N. F. (2000) De novo design of helical bundles as models for understanding protein folding and function, *Acc. Chem. Res. 33*, 745−754.

BI049318K